

Energy Transfer from $\text{NH}(a^1\Delta, \nu)$ to $\text{O}_2(X^3\Sigma_g^-)$: Kinetics of Single Vibrational StatesTh. Martin[†] and F. Stuhl*

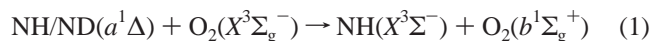
Ruhr-Universität Bochum, Physikalische Chemie I, D-44780 Bochum, Germany

Received: October 6, 2003

This experimental investigation reports the temperature-dependent reaction rate constants for electronically excited, metastable $\text{NH}(a)$ and $\text{ND}(a)$ radicals in the $\nu = 0-3$ levels that are transferring electronic energy to O_2 to yield $\text{O}_2(b)$. The covered temperature range is 209–421 K. All measured Arrhenius activation energies (E_a) are essentially independent of ν and fall into the range of 6.7–9.0 kJ/mol, with an average value of 7.6 kJ/mol, except for $\text{NH}(a, \nu = 3)$, which has an E_a value of 3.5 ± 1.6 kJ/mol. Obviously, for the lowest levels, vibrational excitation does not markedly accelerate the energy transfer and does not seem to be favorable to overcome the small activation barrier. From this and previous work, we propose that a vibrationally adiabatic process generates $\text{NH}(X, \nu)$. In the case of $\text{NH}(a, \nu = 3)$, we suggest that an additional channel opens.

Introduction

Energy transfer reactions among electronically excited states have not been investigated very often, in regard to dependence on their vibrational levels and temperature. In fact, we have not found any references to this subject, except those mentioned here for the metastable imidogen radical, which is isoelectronic with $\text{O}(^1\text{D})$ and $\text{CH}_2(\tilde{a}^1A_1)$. The reaction of metastable $\text{NH}(a^1\Delta)$ and $\text{ND}(a^1\Delta)$ with O_2 , which is the subject of this work, has been previously studied, in regard to its kinetics and its products.^{1–5} It has been shown previously, using quenching and phosphorescence intensity studies at room temperature, that metastable $\text{O}_2(b^1\Sigma_g^+)$ is one of the products



and that the efficiency of this energy transfer process is approximately unity.¹

In the $\nu = 0$ state, this reaction transfers the energy of the highly reactive $\text{NH}(a)$ (151 kJ mol^{-1})⁶ to O_2 , which results in the much more inert, metastable $\text{O}_2(b)$. For the vibrational ground states of both reactants, the energy transfer reaction is slightly endoenergetic (by $\Delta E = 5.14 \text{ kJ mol}^{-1}$), which is well-demonstrated by the different positions of the phosphorescence spectra of both metastable compounds displayed in Figure 2 of ref 1. As a consequence, this is one of the most efficient energy transfer reactions among simple molecules. The room-temperature rate constant for the $\text{NH}(a, \nu = 0)$ level is not very large ($4.9 \times 10^{-14} \text{ cm}^3 \text{ s}^{-1}$).² Activation energies between $8.1 \pm 0.1 \text{ kJ mol}^{-1}$ and $8.66 \pm 0.21 \text{ kJ mol}^{-1}$ have been previously reported for $\nu = 0$ and $\nu = 1$ of $\text{NH}(a)$.^{3,4} For $\nu = 1$, the reaction is exoenergetic already by 33 kJ mol^{-1} , if $\text{O}_2(b^1\Sigma_g^+)$ and $\text{NH/ND}(X^3\Sigma^-)$ are formed in $\nu = 0$. Still, the rate constants at room temperature increase only moderately as ν increases for both $\text{NH}(a)$ and $\text{ND}(a)$,² and the reported activation energies are approximately constant for the two lowest vibrational states of $\text{NH}(a)$.^{3,4} Therefore, the question of whether both products are

generated in $\nu = 0$ for vibrationally excited reactants seems to be debatable.

In the present work, we have studied the kinetics of reaction 1 in the extended vibrational range of $\nu = 0-3$ for both isotopomers in the lower and wider temperature range of 209–421 K. To determine the role of vibration, there are now eight values for the activation barrier available at vibrational energies up to 110 kJ mol^{-1} above the $a, \nu = 0$ states of both isotopomers and at $\sim 105 \text{ kJ mol}^{-1}$ above the resonance energy. Based on this new knowledge, we will discuss the conflicting reports that we have found in the literature on the $\text{NH}(X, \nu)$ quenching product.^{3–5,7} In particular, we will hypothesize on the vibrational levels of both the $\text{NH}(X, \nu)$ and $\text{O}_2(b, \nu)$ products, on the basis of energy considerations.

Experimental Section

The present experimental setup was a modification of that used previously for the studies of the kinetics of $\text{NH/ND}(a)$.^{1,2} NH and ND radicals in the a -state were generated in the photolyses of HN_3 and DN_3 , respectively, using pulsed laser light (repetition frequency of 10–20 Hz) at wavelengths of 193 nm (ArF laser) and, in a few experiments, 248 nm (KrF laser). It has been previously shown that ArF-laser photolysis is one of the most effective methods to generate vibrationally excited, metastable imidogen radicals in the a -state,⁸ as indicated in Table 1 by their relative quantum yields.⁹

The radicals were detected by excitation on the P(2) lines of the $(0 \leftarrow 0)$, $(0 \leftarrow 1)$, $(1 \leftarrow 2)$, and $(1 \leftarrow 3)$ bands of the $\text{NH/ND}(c^1\Pi \leftarrow a^1\Delta)$ absorption transitions using a pulsed dye laser system with the appropriate dyes (Lambda Physik) and frequency doubling for the 320–330 nm region. Subsequent laser-induced fluorescence (LIF) was detected at a spectral bandwidth of 16 nm by a $f = 0.25 \text{ m}$ monochromator monitoring 326-nm light from $\text{NH/ND}(c, \nu = 0)$, 308-nm light from $\text{ND}(c, \nu = 1)$, and 305-nm light from $\text{NH}(c, \nu = 1)$, hence receiving the respective total emission spectra. All these LIF emissions from the $c, \nu = 0$ and $c, \nu = 1$ states lead to the $a, \nu = 0$ levels as the most preferred $c \rightarrow a$ transitions.^{10,11} The $\nu = 0$ level of the $\text{NH}(c)$ state is slightly predissociated and the $\nu = 1$ level is noticeably predissociated.¹² On the other hand, $\text{ND}(c, \nu = 0)$ barely shows predissociation and $\text{ND}(c, \nu = 1)$ shows much less

* Author to whom correspondence should be addressed. E-mail: friedrich.stuhl@ruhr-uni-bochum.de.

[†] Present address: Berufsgenossenschaft der Chemischen Industrie, Kurfürsten-Anlage 62, 69115 Heidelberg, Germany.

TABLE 1: Kinetic Properties of the NH/ND(*a,v*) System, Relevant to Collisions with O₂

	Level, <i>v</i>			
	0	1	2	3
		NH(<i>a,v</i>)		
$\Phi_{\nu,193\text{nm}}^a$	1	0.48 ± 0.11	0.21 ± 0.07	0.13 ± 0.05
$k_{\nu}^E (10^{-14} \text{ cm}^3 \text{ s}^{-1})^b$	4.4 ± 0.5	9.8 ± 2.5	20 ± 14	
$k_{\nu}^Q (10^{-14} \text{ cm}^3 \text{ s}^{-1})^c$	4.9 ± 0.4 ^d 4.3 ± 0.4	8.0 ± 0.7 ^d 8.5 ± 0.4	14.4 ± 2.5 ^d 13.7 ± 0.9	22 ± 7
$A_{\nu} (10^{-12} \text{ cm}^3 \text{ s}^{-1})^e$	0.98 ± 0.015 ^f 1.80 ± 0.10 ^g 1.5 ± 0.4	2.8 ± 0.3 ^f 2.2 ± 0.7	2.3 ± 1.1	1.0 ± 0.5
$E_{a,\nu} (\text{kJ mol}^{-1})^h$	8.1 ± 0.1 ^f 8.66 ± 0.21 ^g 9.05 ± 1.33	8.5 ± 0.6 ^f 7.99 ± 0.9	6.7 ± 1.5	3.5 ± 1.6
		ND(<i>a,v</i>)		
$\Phi_{\nu,193\text{nm}}^a$	1	0.38 ± 0.08	0.16 ± 0.05	0.074 ± 0.029
$k_{\nu}^E (10^{-14} \text{ cm}^3 \text{ s}^{-1})^b$	4.2 ± 0.4	5.3 ± 2.0	0 ± 20	
$k_{\nu}^Q (10^{-14} \text{ cm}^3 \text{ s}^{-1})^c$	3.9 ± 0.5 ^d 2.9 ± 1.1	4.9 ± 0.6 ^d 3.1 ± 1.2	8.3 ± 0.7 ^d 5.3 ± 1.3	10.8 ± 1.5
$A_{\nu} (10^{-12} \text{ cm}^3 \text{ s}^{-1})^e$	0.7 ± 0.5	0.7 ± 0.5	1.5 ± 0.8	1.8 ± 0.8
$E_{a,\nu} (\text{kJ mol}^{-1})^h$	7.3 ± 2.0	7.2 ± 2.3	8.0 ± 1.5	6.7 ± 1.2

^a Relative quantum yield of the production of NH/ND(*a,v*) in the ArF-laser photolyses of HN₃ and DN₃ at 193 nm; from ref 9. ^b Reaction rate constant at ~300 K of the energy transfer to O₂(*b*); from ref 2. ^c Reaction rate constant at ~300 K of the quenching of NH/ND(*a,v*). Further literature data have been discussed in ref 1. ^d From ref 1. ^e Collision factor. ^f From ref 3. ^g From ref 4. ^h Activation energy derived from Arrhenius plot.

predissociation than NH(*c,v* = 1).¹² Because pump and fluorescence wavelengths were chosen to be different (except for the detection of *v* = 0), the amount of stray light was kept small. Decays of relative NH/ND(*a,v*) concentrations were monitored by LIF intensity measurement at 15–20 different delay times between photolysis and analysis lasers, ranging from 10 μs to 2000 μs and, in some cases, 4000 μs. At these delays, the NH/ND(*c*) fluorescence caused by the direct laser photolysis^{8,12} had decayed and did not interfere. The NH/ND(*c*) fluorescence intensity was used as a relative measure of the HN₃/DN₃ concentration.

The photolysis was performed in a stainless-steel vessel that had double walls. It was resistively heated or cooled by cold methanol. This way, a reaction temperature of 209–421 K could be chosen. The photolysis occurred under slow flow conditions. Hydrazoic acid was taken from a 20-L Pyrex bulb, where a mixture of ~0.6% in helium was stored. Oxygen and helium were admixed to this flow. The flow rates were adjusted by mass flow controllers. Finally, the partial pressures of the photolyzed gas mixture were ~3–10 mPa HN₃ or ~2–6 mPa DN₃, 0–250 Pa O₂ in a large excess of helium, up to a total pressure of 3 kPa.

The following chemicals (stated purities; manufacturer) were used: H₂SO₄ (95%–97%; Baker), D₂SO₄ (99.5% purity, 96% in D₂O; Deutero), NaN₃ (>99%; Fluka), helium (99.996%; Messer-Griesheim), and O₂ (99.995%; Messer-Griesheim). Caused by an explosion and in accordance with official safety regulations, we have developed and constructed an automated synthesis procedure to generate HN₃ and DN₃ diluted in a constant flow of helium. Helium was chosen because it did not indicate any vibrational relaxation of NH/ND(*a,v*) that was different from N₂ or argon.²

The HN₃/DN₃ generation occurred outside of, and was well-separated from, the laboratory, in the open. It was housed in a box that had dimensions of 1 m × 1 m × 1 m and 2-mm-thick steel walls. This container was calculated by BAM¹³ to withstand an explosion that involved all the enclosed chemicals. As a further precaution, the steel box was surrounded by

additional large, shielding steel walls at a distance of 1 m from the steel container. The location was inaccessible to persons during the production time. Within the steel box, HN₃/DN₃ was produced by slowly dripping sulfuric acid drop by drop onto sodium azide inside glass equipment, while the reaction zone was flushed with helium at a rate of 85 cm³(STP)/s. The drop rate was adjusted using an electromagnetic dropping funnel and controlled from the laboratory, using a television monitor. The production occurred at atmospheric pressure.

An extrapolation of previous data¹⁴ indicates that hydrazoic acid cannot be ignited at <13% in helium at atmospheric pressure. According to the advice of BAM,¹³ a helium content of 5% should not be exceeded. For further safety, the drop rate was calculated and adjusted to form 1% hydrazoic acid. The mixture of hydrazoic acid and helium was fed into the laboratory through steel tubes 10 m in length and stored in a 20-L glass bulb that was contained in a vented safe box. For purification, the entire system was flushed for 1 h before the 20-L bulb was isolated from the synthesis system, to become the storage facility for the experiments. The production was stopped thereafter. Finally, the reactor was flooded with soda lye and cleaned. Unused hydrazoic azide was destroyed in a pipe that was heated to 440 °C.

Results

The relative efficiency of the hydrazoic acid generation was routinely checked by measuring the NH(*c*) fluorescence intensity directly after the ArF-laser shot.⁸ An NH(*c,v* = 0) lifetime that was similar to the radiative lifetime ($\tau \approx 460 \text{ ns}$)¹² was observed. In practice, the efficiency of the synthesis reaction



was determined by titration to be 0.25–0.4. Fortunately, the quenching of NH(*a*) by helium is very inefficient.¹⁵ In the absence of O₂, the NH/ND(*a*) radicals exhibited lifetimes up to 2 ms, limited mainly by the reaction with hydrazoic acid ($\tau^{-1} = k_{\text{HN}_3}[\text{HN}_3]$)^{15,16} and diffusion in 3 kPa of helium ($\tau^{-1} \approx 350$

s^{-1}), which has been thoroughly studied previously.² Fortunately, the use of this much helium resulted in almost-complete rotational relaxation of the $\text{NH}/\text{ND}(a, \nu)$, which is important to the LIF measurement. The rather-long lifetimes indicated a low degree of impurities, particularly H_2O , which entered the system at each cleaning procedure and will quench HN_3 with high efficiency.¹⁷ Traces of the H_2O impurity and its isotope exchange might have caused the low DN_3/HN_3 production ratio (~ 0.25) found by comparison of the $\text{ND}(c)$ fluorescence intensity with the $\text{NH}(c)$ fluorescence intensity. Although the $\text{ND}(a)$ signal was, hence, much smaller, the $\text{ND}(a)$ kinetics could be followed without interference from $\text{NH}(a)$, because of the good spectral resolution of the LIF method.

Quenching rate constants, $k_v^Q(T)$, of level ν were derived at temperature T from lifetime measurements of $\text{NH}/\text{ND}(a, \nu)$. The lowest and highest temperatures were in the ranges of 209–217 K and 384–421 K, respectively, for all eight $\text{NH}/\text{ND}(a, \nu)$ reactants. The lifetimes were checked to be insensitive to changes of the (i) photolysis wavelengths (193 and 248 nm), (ii) LIF pumping lines [$\text{NH}(a, \nu = 1, \text{Q}(2), \text{Q}(4), \text{P}(2, 3, \text{and } 5))$], (iii) total pressures [2.5–3.5 kPa helium for $\text{NH}(a, \nu = 1)$], and (iv) HN_3 pressures (3.3–33 Pa).

Values of $k_v^Q(T)$ were determined at 8–15 different temperatures for each of the four $\text{NH}(a, \nu)$ levels and at 5–7 temperatures for $\text{ND}(a, \nu)$. At each temperature, the $\text{NH}/\text{ND}(a, \nu = 0-3)$ decays were monitored typically at 6–8 different O_2 concentrations, as described in the Experimental Section. Each decay curve consisted of ~ 15 data points on the time scale. Within the precision of this work, all decays were observed to be exponential defining decay rates, τ^{-1} . These rates were plotted against the concentration of O_2 , according to the relation $\tau^{-1} = \tau_0^{-1} + k_v^Q(T)[\text{O}_2]$. The parameter τ_0^{-1} represents the lifetime of $\text{NH}/\text{ND}(a, \nu)$ at zero pressure of O_2 . The useful O_2 concentration range was limited in the studies of $\text{NH}(a, \nu = 0$ and $\nu = 1)$ and $\text{ND}(a, \nu)$, because of effective quenching of the c -state levels by O_2 .^{18–21} The values of $k_v^Q(T \approx 300 \text{ K})$ obtained from plots of τ^{-1} vs $[\text{O}_2]$ are listed in Table 1, in comparison with values reported previously from our laboratory for the quenching (k_v^Q) and the energy transfer to $\text{O}_2(b)$ (k_v^E), which have been previously investigated by $\text{NH}/\text{ND}(a)$ - and $\text{O}_2(b)$ -phosphorescence intensity measurements.¹ They all agree within the given error limits, confirming, in particular, that the efficiency of the energy transfer to $\text{O}_2(b)$ is almost 1; i.e., the phrases quenching, energy transfer, and even intersystem crossing rate constants mean the same in this case. The rate constants at room temperature are smaller for the isotopomer ND and increase slightly less than those for NH as ν increases, although the isotope effect is not spectacular, considering the much smaller vibrational energy gaps of $\text{ND}(a)$.

The temperature-dependent rate constants are then plotted in Arrhenius representations, i.e., $\ln\{k_v^Q(T)/(\text{cm}^3 \text{ s}^{-1})\}$ vs $(T/\text{K})^{-1}$, according to the relation $k_v^Q(T) = A_\nu e^{-E_{a,\nu}/(RT)}$. The Arrhenius plots are displayed in Figures 1 and 2 for $\text{NH}(a, \nu)$ and $\text{ND}(a, \nu)$, respectively. At a first glance, one notices that the data for $\text{NH}(a, \nu = 0$ and $\nu = 1)$ are much more precise than those for $\text{ND}(a, \nu = 0$ and $\nu = 1)$. This is caused by the low DN_3 yield. On the other hand, the detection of $\text{ND}(a, \nu = 2$ and $\nu = 3)$ was favorable because of the longer lifetime of $\text{ND}(c, \nu = 1)$. Common to all data for the deuterated species were the fewer number of lifetime measurements, because the purpose was to determine differences between the deuterated and hydrogenated systems rather than precise data for $\text{ND}(a, \nu)$.

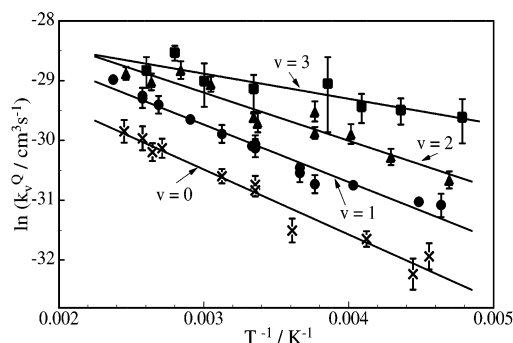


Figure 1. Arrhenius plots $\ln\{k_v^Q(T)/(\text{cm}^3 \text{ s}^{-1})\}$ vs $(T/\text{K})^{-1}$ for the quenching of $\text{NH}(a)$ in the various vibrational states $\nu = 0-3$: (\times) $\nu = 0$, (\bullet) $\nu = 1$, (\blacktriangle) $\nu = 2$, and (\blacksquare) $\nu = 3$.

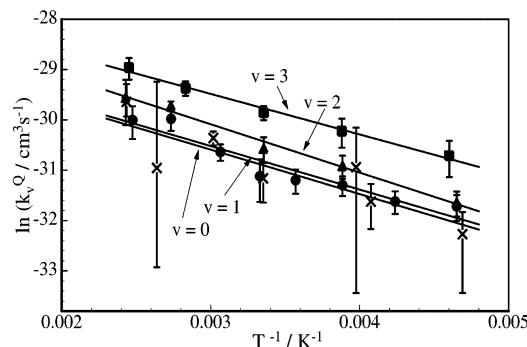


Figure 2. Arrhenius plots $\ln\{k_v^Q(T)/(\text{cm}^3 \text{ s}^{-1})\}$ vs $(T/\text{K})^{-1}$ for the quenching of $\text{ND}(a)$ in the various vibrational states $\nu = 0-3$: (\times) $\nu = 0$, (\bullet) $\nu = 1$, (\blacktriangle) $\nu = 2$, and (\blacksquare) $\nu = 3$.

Discussion

The quantum yield of $\text{NH}(a)$ in the photolysis of HN_3 has been reported previously⁸ to be $\Phi \approx 0.4$. The formation of vibrationally excited states has been established in several studies.^{3,8,10,22} Literature values of the relative quantum yields for vibrational excitation (Φ_ν), given in Table 1, show that vibrationally excited $\text{ND}(a, \nu)$ are less efficiently generated than $\text{NH}(a, \nu)$,⁹ favoring the detection of the hydrogenated species. $\text{NH}(a, \nu = 0$ and $\nu = 1)$ are reported to be formed rotationally hot with $T_{\text{rot}} = 3150$ and 2450 K , respectively.⁸ Previously, it has been shown² (and was confirmed in this work) that the radicals are rotationally but not vibrationally relaxed by 3 kPa of helium, so that the LIF measurement of one rotational level is representative for all rotational levels.

Basically, three different processes can be made responsible for the removal of vibrationally excited imidogen radicals in the a -state: (i) quenching to yield products other than $\text{O}_2(b)$; (ii) resonance energy transfer to $\text{O}_2(b)$, as given by reaction 1; and (iii) vibrational relaxation for the levels $\nu > 0$. We observe significant increases in the rate constants with increasing ν in Table 1. This could be, in fact, due to an enhanced removal of the vibrationally excited states by relaxation to lower vibrational states. However, we believe that there are two reasons why vibrational relaxation is a minor process:

(1) As already mentioned, the previous kinetic and phosphorescence intensity measurements¹ indicate that the energy transfer occurs with an efficiency that is similar to unity.

(2) Because no deviation from exponential decays is observed in the presence of O_2 in this and previous work from our laboratory,² vibrational relaxation seems to be a minor process, which is in agreement with the work of other researchers.^{3,7}

On the other hand, deviation from exponential decays have been clearly observed during the removal of $\text{NH}(a, \nu > 0)$ by

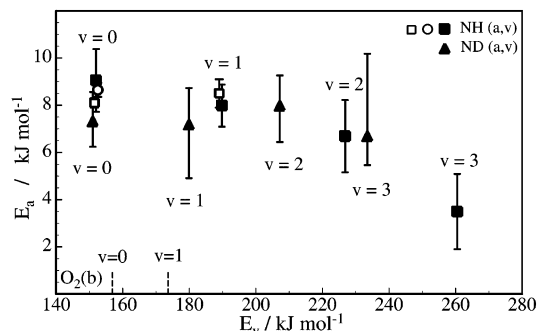


Figure 3. Measured activation energy (E_a) plotted as a function of the energy of the vibrational states of NH/ND(a,v) (E_v). Zero energy is the lowest rotational level of $v = 0$ of the ground-state NH/ND(X) radicals. Also displayed are the reported values of (\square) ref 3 and (\circ) ref 4. Included are the vibrational energies of $O_2(b, v = 0$ and 1).

N_2 , and relaxation rate constants have been previously deduced for the relaxation reactions.^{2,8} The facts mentioned under reasons (1) and (2) were established for $T = 300$ K; hence, our assumption here is that they also are valid for the entire temperature range presented. After all, the increase of k_v^Q with increasing v (Table 1) is not well understood: It might be, at least partly, due to the increasing size of a vibrating radical.

The values of the Arrhenius parameters, A_v and $E_{a,v}$, which we have deduced from Figures 1 and 2, are listed in Table 1, together with the values reported by Morgenroth³ and Nelson et al.⁴ The present values of A_v vary from $2.3 \times 10^{-12} \text{ cm}^3 \text{ s}^{-1}$ to $1.0 \times 10^{-12} \text{ cm}^3 \text{ s}^{-1}$ for NH(a,v) and from $1.8 \times 10^{-12} \text{ cm}^3 \text{ s}^{-1}$ to $0.7 \times 10^{-12} \text{ cm}^3 \text{ s}^{-1}$ for ND(c,v). In the simple Arrhenius representation, this does not tell us much about the barrier and will be discussed below only briefly. For small activation energies (as encountered in this work), one must remember that $E_{a,v}$ represents only an approximate measure of the reaction barrier. Therefore, we will discuss the trend rather than the absolute value. In Figure 3, the derived values of $E_{a,v}$ are presented as a function of the energy of the vibrational states, as measured from the NH/ND($X, v = 0$) ground states. Included in the figure are the values of Morgenroth³ and Nelson et al.⁴ for NH($a, v = 0$ and $v = 1$). Also shown are the positions of $v = 0$ and $v = 1$ of $O_2(b)$. Several features are noteworthy in this figure:

(1) The present values agree very well with the literature values.^{3,4}

(2) The $E_{a,v}$ values seem to be constant up to $v = 2$ of NH(a) and $v = 3$ of ND(a), which have approximately the same energy.

(3) At the highest vibrational energy (namely, $v = 3$ of NH(a)), the $E_{a,v}$ value seems to decrease.

(4) The endothermicities for the $v = 0$ levels, as well as the exothermicities for the higher vibrational levels, are evident, provided that NH(X) is formed in the vibrational ground state ($v = 0$), as assumed in Figure 3.

(5) The energetic position of $O_2(b, v = 1)$ does not seem to influence the values of the activation energies. Without further compelling proof, we therefore propose $O_2(b, v = 0)$ to be one of the products.

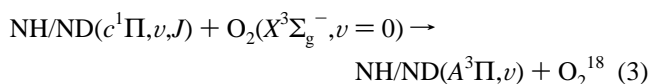
The apparent invariance of the barrier height mentioned under feature (2) implies that increasing A_v factors is a reason for the rate constants to increase as v increases, as supported from the data in Figures 1 and 2 and in Table 1. In the simplest Arrhenius model, the A_v factor is determined by the size of the molecule, i.e., by vibrational expansion of the radicals, as hypothesized above.

The present work does not determine the vibrational excitation of the other product, NH(X, v). One finds conflicting results on this matter in the literature. Morgenroth³ recently did not observe NH($X, v > 0$) and concluded that vibrationally excited NH(a, v) are deactivated solely to NH($X, v = 0$). This fact contradicts earlier observations in the 193-nm photolysis of HNC O .⁷ Drozdowski et al.⁷ found, in the presence of O_2 , that the yield of NH($X, v = 1$) is 18% of that of $v = 0$ with some evidence for $v = 2$. Currently, we know that the photolysis yield was $\sim 26\%$ in NH($a, v = 1$) and 3% in NH($a, v = 2$).⁹ In the presence of O_2 , Nelson et al.⁴ observed NH($X^3\Sigma^-$) that contained multiple quanta of vibrational energy as a primary product. Moreover, Adams and Pasternack⁵ observed similar rate constants for the removal of NH(a, v) and the appearance of NH(X, v) for all levels of $v = 0-2$. They concluded that the more rapidly quenched, higher vibrational levels of NH($a^1\Delta$) would be required to populate the higher vibrational levels of NH($X^3\Sigma^-$).⁷ On the other hand, the relative production yield of $v > 0$ in the presence of O_2 proved to be significantly lower than the yield in the presence of xenon, which previously has been shown to quench NH(a, v) vibrationally adiabatic.^{5,23,24} Adams and Pasternack⁵ also showed that the removal rates of NH(X, v) are relatively large; however, they mentioned that this has been taken into account. In the case that reaction 1 leads exclusively to NH($X, v = 0$), the barrier would seem to be invariant within a reaction enthalpy range from $+5 \text{ kJ mol}^{-1}$ to -70 kJ mol^{-1} , as displayed by the data of Figure 3. Conversely assuming vibrational adiabaticity, the endothermicity would change by only $\sim 1 \text{ kJ mol}^{-1}$, i.e., remain essentially constant for the reactions of NH($a, v = 0-2$) and ND($a, v = 0-3$). All these arguments lead us to believe that a conservation of vibration during the intersystem crossing process occurs to a significant extent. This means that the vibration in the a -state acts as a spectator during the energy transfer, in which no bond is broken and no new bond is formed.

In their previous investigation of the NH($a, v = 0$) + O_2 reaction, Nelson et al.⁴ observed an appreciable activation energy for the first time. By analogy to the quenching by N_2 , which they considered in detail in that work, they attributed the activation energy to a barrier in the entrance channel for complex formation. If our presumption of a vibrationally adiabatic process is true, this complex must be sufficiently loose and/or short-lived to preserve the vibration.

A notable trend seems to appear for NH($a, v = 3$), in regard to the decreased activation energy. Unfortunately, because of the insufficient detection sensitivity, we were not able to study higher vibrational levels for further confirmation of this trend. NH($a, v = 3$) lies slightly above the NH($b^1\Sigma^+, v = 0$) state and collision-induced curve crossing must be considered, among other possibilities.

We will finally mention that another O_2 -induced intersystem crossing process has been previously observed for a different, electronically excited, singlet NH/ND state, namely



In that case, the primary intention was to study the rotational dependence, and, therefore, this system is kinetically more complex than reaction 1. The vibrational distribution in the NH/ND(A) product is distinctly different from that observed for the present process, although there is a propensity for the population of $v = 0$ from $v = 0$. However, at increasing levels of J , the formation of NH($A, v = 2$) is the major product from NH($c, v =$

0, J), for example. Also, for reaction 3, it has been discussed whether energy resonances play a role.

Acknowledgment. We thank Dr. Christian Lotz for preliminary experiments. Financial support from the Deutsche Forschungsgemeinschaft (Stu59/37-1 and Stu59/37-2) and Fonds der Chemischen Industrie is gratefully acknowledged. We also thank the Bundesanstalt für Materialforschung und -prüfung in Berlin (BAM) for advising us to construct a safe synthesis method for hydrazoic acid.

References and Notes

- (1) Bohn, B.; Stuhl, F. *J. Phys. Chem.* **1995**, *99*, 965.
- (2) Bohn, B.; Stuhl, F. *J. Phys. Chem.* **1993**, *97*, 7234.
- (3) Morgenroth, K.-H. Dissertation, Mathematisch-Naturwissenschaftliche Fakultäten der Georg-August-Universität zu Göttingen, Göttingen, Germany, 1996.
- (4) Nelson, H. H.; McDonald, J. R.; Alexander, M. H. *J. Phys. Chem.* **1990**, *94*, 3291.
- (5) Adams, J. S.; Pasternack, L. *J. Phys. Chem.* **1991**, *95*, 2975.
- (6) Rinnenthal, J. L.; Gericke, K.-H. *J. Mol. Spectrosc.* **1999**, *198*, 115.
- (7) Drozdowski, W. S.; Baronavski, A. P.; McDonald, J. R. *Chem. Phys. Lett.* **1979**, *64*, 421.
- (8) Rohrer, F.; Stuhl, F. *J. Chem. Phys.* **1988**, *88*, 4788.
- (9) Bohn, B.; Stuhl, F. *J. Phys. Chem.* **1993**, *97*, 4891.
- (10) Nelson, H. H.; McDonald, J. R. *J. Chem. Phys.* **1990**, *93*, 8777.
- (11) Hack, W.; Mill, Th. *J. Phys. Chem.* **1993**, *97*, 5599.
- (12) Bohn, B.; Stuhl, F.; Parlant, G.; Dagdigian, P. J.; Yarkony, D. R. *J. Chem. Phys.* **1992**, *96*, 5059.
- (13) BAM, Bundesanstalt für Materialforschung und -prüfung, D-12200 Berlin, Germany.
- (14) Rozenberg, A. S.; Voronkov, V. G. *Russ. J. Phys. Chem.* **1969**, *43*, 1333.
- (15) Rohrer, F.; Stuhl, F. *Chem. Phys. Lett.* **1984**, *111*, 234.
- (16) Freitag, F.; Rohrer, F.; Stuhl, F. *J. Phys. Chem.* **1989**, *93*, 3170.
- (17) Hack, W.; Jordan, R. *Ber. Bunsen-Ges.* **1997**, *101*, 545.
- (18) Hohmann, J.; Stuhl, F. *J. Phys. Chem. A* **1997**, *101*, 5607.
- (19) Rohrer, F.; Stuhl, F. *J. Chem. Phys.* **1987**, *86*, 226.
- (20) Kenner, R. D.; Rohrer, F.; Stuhl, F. *J. Phys. Chem.* **1989**, *93*, 7824.
- (21) Kenner, R. D.; Pfannenberger, S.; Heinrich, P.; Stuhl, F. *J. Phys. Chem.* **1991**, *95*, 6585.
- (22) Kenner, R. D.; Rohrer, F.; Stuhl, F. *J. Chem. Phys.* **1987**, *86*, 2036.
- (23) Hack, W.; Rathmann, K. *J. Phys. Chem.* **1992**, *96*, 47.
- (24) Patel-Misra, D.; Dagdigian, P. J. *J. Chem. Phys.* **1992**, *97*, 4871.